Physica B 404 (2009) 4354–4358

Contents lists available at ScienceDirect

Physica B

journal homepage: www.elsevier.com/locate/physb

The silicon vacancy in SiC

Erik Janzén [a,*], Adam Gali [b], Patrick Carlsson [a], Andreas Gällström [a], Björn Magnusson [a,c], N.T. Son [a]

[a] Department of Physics, Chemistry and Biology, Linköping University, SE-581 83 Linköping, Sweden
[b] Department of Atomic Physics, Budapest University of Technology and Economics, Budafoki út 8, H-1111 Budapest, Hungary
[c] Norstel AB, Ramshällsvägen 15, SE-602 38 Norrköping, Sweden

ARTICLE INFO

PACS:
61.18.Fs
61.72.Bb
61.72.Jd
61.72.Ji

Keywords:
Silicon vacancy
SiC
EPR
ODMR
PL

ABSTRACT

The isolated silicon vacancy is one of the basic intrinsic defects in SiC. We present new experimental data as well as new calculations on the silicon vacancy defect levels and a new model that explains the optical transitions and the magnetic resonance signals observed as occurring in the singly negative charge state of the silicon vacancy in 4H and 6H SiC.

© 2009 Elsevier B.V. All rights reserved.

1. Introduction

The isolated silicon vacancy (V_{Si}) is one of the basic intrinsic defects in SiC. Due to the existence of inequivalent Si lattice sites there are in 4H SiC two V_{Si}, one hexagonal (h) and one quasi-cubic (k); while in 6H SiC there are three V_{Si}, one hexagonal (h) and two quasi-cubic (k_1 and k_2), each of them having several different charge states in the band gap. The reported photoluminescence (PL) and magnetic resonance signals attributed to V_{Si} are not conclusive concerning the origin, site, charge state etc of this defect.

We will here present (1) new experimental data as well as (2) new calculations on the V_{Si} defect levels and (3) a new model that explains the optical transitions and the magnetic resonance signals observed as occurring in the singly negative charge state of the silicon vacancy (V_{Si}^{-}) in 4H and 6H SiC.

2. Experimental and calculations

Optical spectroscopy. The samples have been investigated using Fourier transform infrared spectroscopy (FTIR) absorption. We have also measured the PL using a single monochromator and a multichannel CCD detector. In the PL experiments the samples were excited with a Ti:Sapphire laser at 752.5 nm.

Magnetic resonance. Optical detection of magnetic resonance (ODMR) experiments were performed on a modified X-band (∼9.23 GHz) Bruker spectrometer. The UV multi-lines of an ion Ar laser were used for excitation. For resonance excitation, a tuneable Ti:Sapphire laser was used. Electron paramagnetic resonance (EPR) experiments were carried out on an X-band E580 Elexsys spectrometer. The sample temperature could be regulated between 5 K and room temperature.

Calculations. The calculations have been carried out in a large 576-atom supercell using the Γ-point for k-point sampling. We could describe the localized defect states accurately. The Γ-point was needed to maintain the degenerate states, while the charge density was convergent in this large supercell at the same time. We have used density functional theory within local density approximation for the Hamiltonian which gives reliable order of the one-electron defect levels.

3. Previous results

There are two main no-phonon PL lines V1 and V2 in 4H SiC and three V1, V2 and V3 in 6H SiC that are related to V_{Si} [1,2], see Fig. 1. For both polytypes V1 has a high temperature companion V1′. No V2′ or V3′ lines have been observed. All PL lines are also visible in absorption. The lines were reported not to split in magnetic field [2]. At low temperatures two ODMR signals (T_{V1a}, T_{V1b} and so on) could be detected via each PL line. All ODMR signals were reported to be triplets (S=1) with isotropic g values

* Corresponding author.
E-mail address: erija@ifm.liu.se (E. Janzén).

0921-4526/$ - see front matter © 2009 Elsevier B.V. All rights reserved.
doi:10.1016/j.physb.2009.09.023

close to 2. By selective excitation in each line, only the “a” ODMR signal of that line could be detected [1]. The polarization dependence of several of the lines was not conclusive. Later it was unambiguously shown that the T_{V2a} signal in 4H SiC had $S=3/2$ [3,4] and that it could be detected by EPR in darkness in some samples [5]. In addition, another EPR center with negligible zero-field splitting and $S=3/2$ was reported as V_{Si}^{-} in Ref. [6].

4. The model

In the V_{Si}, four C dangling bonds point to the vacant site. The bonds are too localized to overlap. Instead, the C atoms relax outwards and basically keep the C_{3v} symmetry independently of its charge state or its site in 4H SiC. The dangling bonds form two a_1 (degeneracy 2 if spin is included) levels and one e (degeneracy 4 if spin is included) level. The first a_1 level is resonant with the valence band not far from the top of it, while the remaining a_1 and e levels are very close (a_1 below e) at around 0.5–0.7 eV above the valence band edge in the neutral charge state increasing to about 0.9 eV in the singly negative charge state V_{Si}^{-}. In V_{Si}^{-}, there are five electrons distributed among the a_1, a_1 and e one-electron levels, (Fig. 2). The possible multiplets are listed in Table 1. If there are two electrons in the lowest a_1 level resonant with the valence band, one electron in the next a_1 level and two electrons in the e level, the electronic configuration can be denoted as $a_1^2a_1^1e^2$.

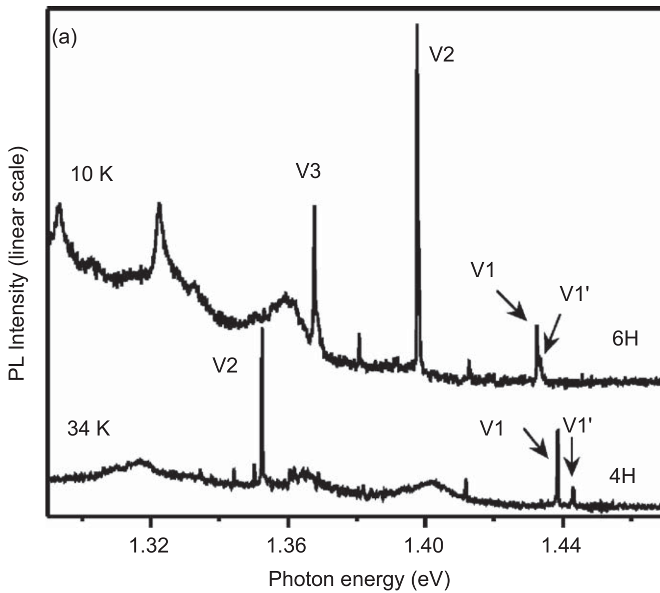

Fig. 1. Silicon vacancy related PL lines in 4H and 6H SiC (from Ref. [2]).

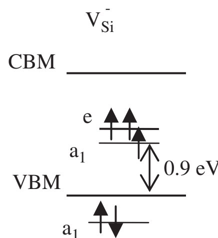

Fig. 2. The spins of the three electrons in the band gap in the singly negative charge state of the silicon vacancy line ($S=3/2$) in the ground state $^4A_2$.

Keeping the lowest a_1 level full yields the only configuration that allows a high-spin ($S=3/2$) multiplet state $^4A_2$, which is also expected to be the ground state. This is experimentally confirmed by the EPR observation of T_{V2a} in darkness.

The a_1 and e levels in the band gap are so close that it is relevant to consider also the T_d case when they have merged to a t_2 (degeneracy 6 if spin is included) level. The possible multiplets in that case are also listed in Table 1. The energy separation between the different multiplets originating from the same electronic configuration is expected to be 0.5–1 eV in the T_d case, which is only slightly smaller than the expected energy separation between different electronic configurations. The additional splitting of the multiplets induced by the hexagonal field going from T_d to C_{3v} symmetry will be much smaller.

In principle all multiplets with the same symmetry label in Table 1 will mix. For instance, there are two $^4A_2$ multiplets: $^4A_2(a_1^2a_1^1e^2)$ and $^4A_2(a_1^1a_1^2e^2)$. Interaction between them will increase their energy separation and thus lower the energy of the $^4A_2$ multiplet with the lowest energy. However, if the energy separation between the multiplets is large the effect will be small. In the same way low-lying doublets, (see Table 1), may be pushed down by interaction with higher-lying doublets of the same symmetry. As mentioned above, we find experimentally that the high-spin state is the ground state for V_{Si}^{-}.

5. Optical selection rules

An optical transition between an initial and final state having the same spin S is allowed if the direct product $\Gamma_{initial}\otimes\Gamma_d\otimes\Gamma_{final}$ contains A_1. In C_{3v} symmetry $\Gamma_{initial}$ and Γ_{final} are either A_1, A_2 or E. Γ_d is A_1 for light polarized parallel to the *c* axis and E for light

Table 1
Possible multiplets formed by the five electrons in V_{Si}^{-} in different electronic configurations in C_{3v} and T_d symmetry.

Electronic configuration		Possible multiplets
C_{3v}	T_d	
$a_1^2a_1^2e^1$		^2E
$a_1^2a_1^1e^2$		$^4A_2$, $^2A_2$, ^2E, $^2A_1$
$a_1^1a_1^0e^3$		^2E
	$a_1^2t_2^3$	$^4A_2$, $^2T_1$, ^2E, $^2T_2$
$a_1^1a_1^2e^2$		$^4A_2$, $^2A_2$, ^2E, $^2A_1$
$a_1^1a_1^1e^3$		^4E, ^2E, ^2E
$a_1^1a_1^0e^4$		$^2A_1$
	$a_1^1t_2^4$	$^4T_1$, $^2T_1$, ^2E, $^2T_2$, $^2A_1$
$a_1^0a_1^2e^3$		^2E
$a_1^0a_1^1e^4$		$^2A_1$
	$a_1^0t_2^5$	$^2T_2$

Table 2
Optical transitions between multiplets in C_{3v} symmetry.

$\Delta S=0$	A_1	A_2	E
A_1	∥	0	⊥
A_2		∥	⊥
E			∥, ⊥

∥: allowed if polarized ∥*c* axis, ⊥: allowed if polarized ⊥*c* axis, 0: forbidden.

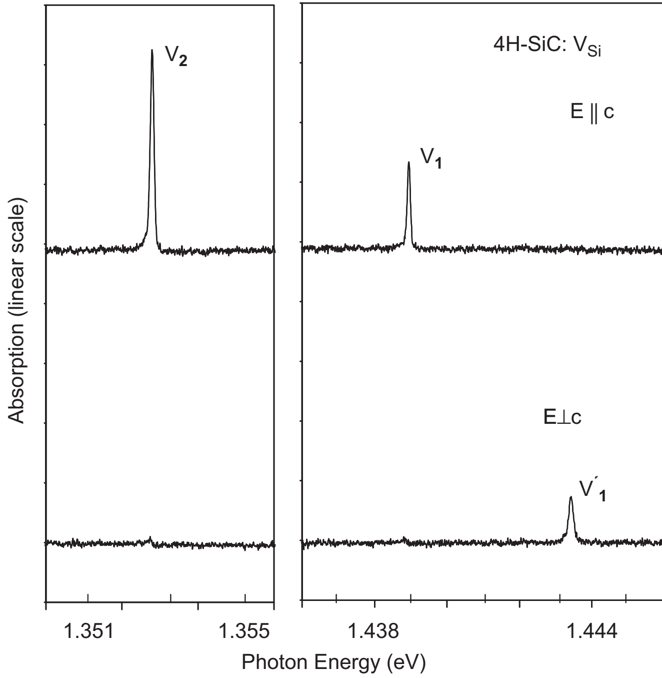

Fig. 3. Polarization dependence of silicon vacancy related absorption lines in 4H SiC.

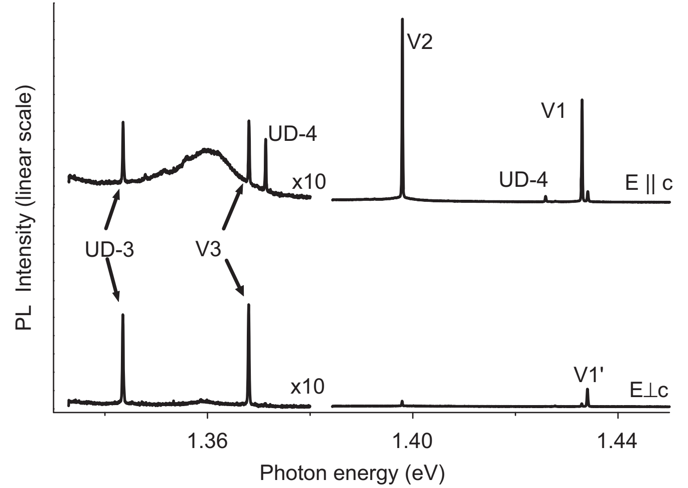

Fig. 4. Polarization dependence of silicon vacancy related PL lines in 6H SiC.

polarized perpendicular to the *c* axis. The allowed, as well as the forbidden transitions are shown in Table 2. If the two states have different spins, the optical transition between them is forbidden in the first order.

6. Experimental results and discussions

Optical. Since the PL lines shown in Fig. 1 also are observed in absorption, the optical transitions must be allowed. Assuming that the ground state is $^4A_2(a_1^2a_1^1e^2)$ the only allowed transitions in C_{3v} symmetry are to excited $^4A_2$ (polarized ∥c) and ^4E (polarized ⊥c) states, see Table 2. The only way of getting an excited $^4A_2$ state is to transfer an electron from the lowest a_1 level resonant with the valence band to the upper a_1 level in the gap $^4A_2(a_1^1a_1^2e^2)$, see Table 1; if the electron instead is transferred to the e level in the gap we get $^4E(a_1^1a_1^1e^3)$. In Figs. 3 and 4 the polarization dependence of the absorption and PL lines V1, V1′ and V2 in 4H SiC and V1, V1′, V2 and V3 in 6H SiC, respectively, is shown. In the proposed model we can clearly assign V1 and V2 to the transition $^4A_2(a_1^2a_1^1e^2)\rightarrow{}^4A_2(a_1^1a_1^2e^2)$ at different sites and V1′ to $^4A_2(a_1^2a_1^1e^2)\rightarrow{}^4E(a_1^1a_1^1e^3)$. V3 does not have a clear polarization dependence which indicates that $^4A_2(a_1^1a_1^2e^2)$ and $^4E(a_1^1a_1^1e^3)$ are very close for this site (<0.1 meV). The optical results are summarized in Fig. 5.

ODMR. The two previously reported ODMR signals related to each of the V1, V2 and V3 lines [1] can then be assigned to the initial and final states of the transitions, respectively, for instance, T_{V2a} to the ground state $^4A_2(a_1^2a_1^1e^2)$ and T_{V2b} to the excited state $^4A_2(a_1^1a_1^2e^2)$ of the V2 transition. The PL lines will not split in a magnetic field, since it is experimentally found that both the ground and excited states have the same spin and *g* values and optical transitions are only allowed between substates having the same *Ms* value.

Only the $^4A_2$ states will give rise to ODMR signals, since the zero-field splitting due to spin–orbit interaction of ^4E states is so large that the microwave (MW) field cannot induce transitions between the substates for normal magnetic fields.

EPR. The $^4A_2$ ground state will split due to spin–spin interaction into one doublet state Γ_4 ($Ms=\pm1/2$) and two degenerate singlet states Γ_5 and Γ_6 ($Ms=\pm3/2$), (Fig. 6). The two singlets are coupled to each other due to time-reversal symmetry. The separation is the zero-field splitting 2D and is less than a μeV. In T_d symmetry $D=0$. When a magnetic field **B** is applied, further splitting into four substates occurs. If **B**∥**c** the energies of the four substates are given by

$$E(Ms=\pm3/2)=E_0+D+Msg\mu_BB. \quad (1)$$

$$E(Ms=\pm1/2)=E_0-D+Msg\mu_BB. \quad (2)$$

where E_0 is the energy of the unsplit $^4A_2$ state (Fig. 6). A MW field of frequency ν can induce transitions between substates separated by $h\nu$ if $\Delta Ms=\pm1$. (10 GHz corresponds to about 40 μeV). This will happen when the magnetic field is B_1 ($Ms=+3/2\leftrightarrow Ms=+1/2$), B_2 ($Ms=+1/2\leftrightarrow Ms=-1/2$) and B_3 ($Ms=-1/2\leftrightarrow Ms=-3/2$) in Fig. 6. From Eqs. (1) and (2) we can easily deduce that $B_2=h\nu/(g\,\mu_B)$ and $B_{3,1}=B_2\pm2D/(g\,\mu_B)$. In EPR the induced transitions are detected as a change in the intensity of the reflected wave while varying the magnetic field. The magnetic field separation between the EPR signals is thus a measure of the zero-field splitting.

A typical EPR spectrum in darkness of silicon vacancy related defects in 4H SiC is shown in Fig. 7. In previous studies, the T_{V2a} signals were not reported and only the central line was detected [6]. The central structure is very similar to the EPR signature of V_{Si}^- in 3C SiC [7] and was interpreted as a V_{Si}^- related defect with negligible zero-field splitting [6], although the assumed hyperfine interactions (HF) with the neighboring 12 Si atoms seem to be too large (b/a is 40% instead of the 25% calculated from the natural abundance of ^{29}Si). The outer structures are due to T_{V2a}; its third line ($Ms=+1/2\leftrightarrow Ms=-1/2$ in Fig. 5) is within the central V_{Si}^- structure. There are no signs of T_{V1a} or any of the other signals observed in ODMR. For 6H SiC the situation is similar. Only T_{V2a}, T_{V3a} and a V_{Si}^- related defect with negligible zero-field splitting are visible.

We have used low MW powers and low modulation fields to considerably improve the EPR resolution. From the high-resolution EPR spectrum in Fig. 8 it is obvious that the V_{Si}^- related defect with negligible zero-field splitting does not exist. Instead the central structure is due to (1) the central lines of T_{V1a} and T_{V2a}

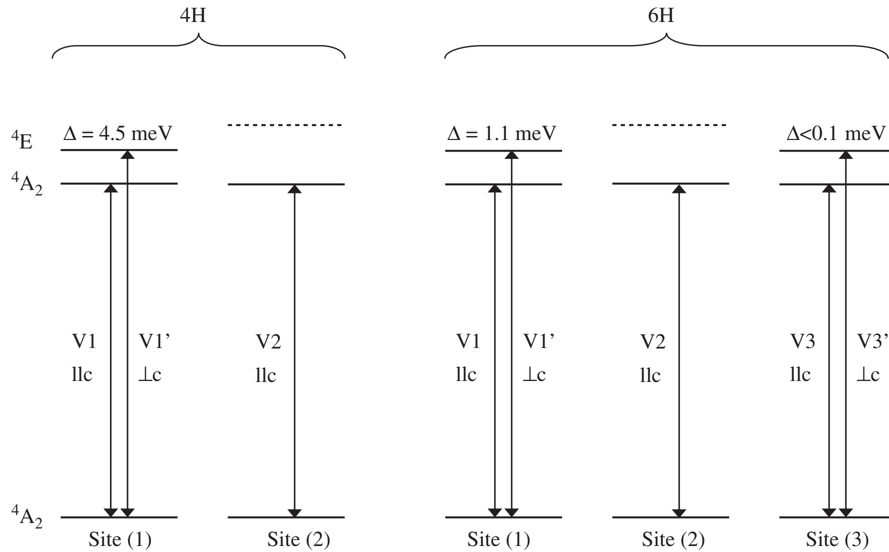

Fig. 5. The internal optical transitions of V_{Si}^- in 4H and 6H SiC.

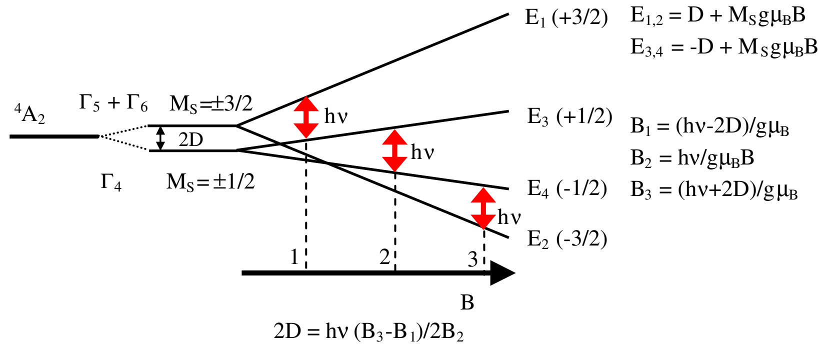

Fig. 6. Splitting of a $^4A_2$ state in C_{3v} symmetry by spin–spin interaction and magnetic field in the c direction.

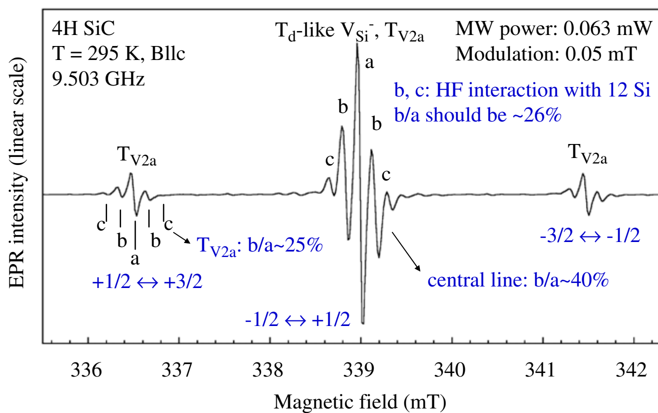

Fig. 7. Low-resolution EPR spectra of T_{V2a} and V_{Si}^- in 4H SiC measured at 293 K for **B**∥**c** with the MW power of 0.063 mW and a field modulation of 0.05 mT.

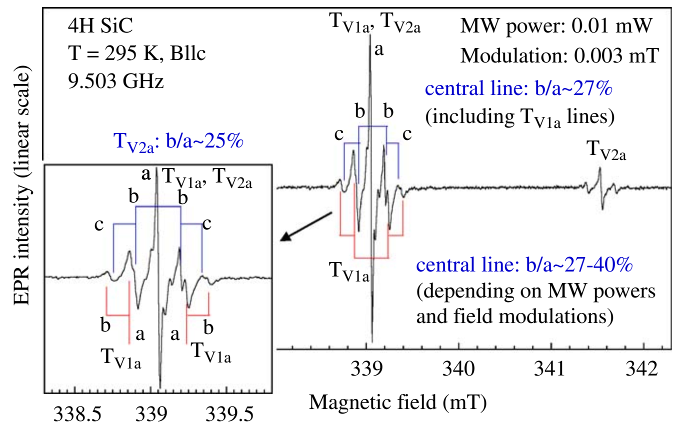

Fig. 8. High-resolution EPR spectra of T_{V1a} and T_{V2a} in 4H SiC measured at 293 K for **B**∥**c** with MW power of 0.01 mW and a field modulation of 0.003 mT. With a line width of ~0.02 mT, the usual hyperfine structure of the central line is shown to be due to overlapping between the hyperfine structure of the 12 next-nearest Si neighbor and other lines corresponding to the transitions between the spin states $+1/2 \leftrightarrow +3/2$ and $-1/2 \leftrightarrow -3/2$ of the T_{V1a} center.

($Ms=+1/2 \leftrightarrow Ms=-1/2$), (2) the lines ($Ms=+3/2 \leftrightarrow Ms=+1/2$) and ($Ms=-1/2 \leftrightarrow Ms=-3/2$) of T_{V1a} (marked a) and (3) hyperfine interactions with the 12 next-nearest Si neighbors (marked b and c). From the angular dependence (not shown here) we get an isotropic g value of 2.0028 for both T_{V1a} and T_{V2a}. Similarly for 6H SiC, (Fig. 9) all structures can be explained by the different lines of T_{V1a}, T_{V2a} and T_{V3a}, which all have an isotropic g value of 2.0026. The zero-field splittings of the ground and excited $^4A_2$ states of V_{Si}^-

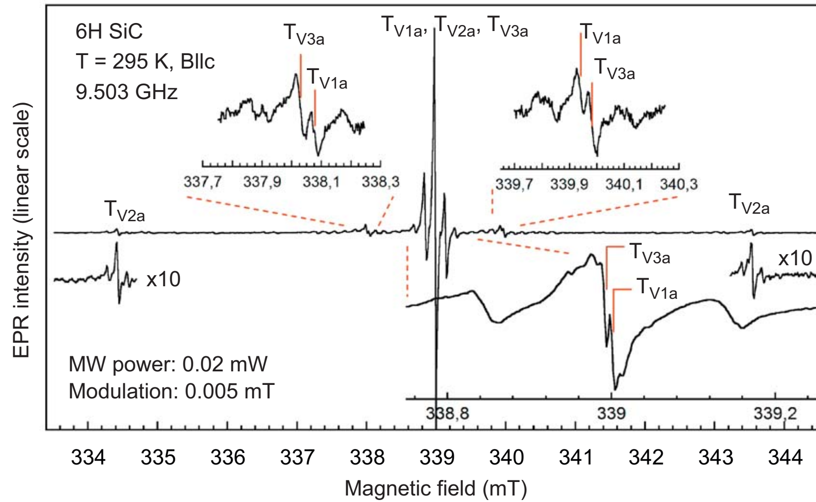

Fig. 9. High-resolution EPR spectra of T_{V1a},T_{V2a} and T_{V3a} in 6H SiC measured at 293 K for **B**||**c** with the MW power of 0.02 mW and a field modulation of 0.005 mT. EPR lines corresponding to the transitions between the spin states $+1/2 \leftrightarrow +3/2$, $-1/2 \leftrightarrow +1/2$ and $-1/2 \leftrightarrow -3/2$ of the T_{V1a} and T_{V3a} centers are resolved.

	4H		6H			
$^4A_2$	T_{V1b}	T_{V2b}	T_{V1b}	T_{V2b}	T_{V3b}	
	0.25 μeV	0.15 μeV	0.26 μeV	0.08 μeV	0.24 μeV	ODMR data
	$^4A_2$, ^4E close		$^4A_2$, ^4E close		$^4A_2$, ^4E close	
	k	***h***	k_1	***h***	k_2	
	0.02 μeV	0.29 μeV	0.11 μeV	0.53 μeV	0.12 μeV	EPR data
$^4A_2$	T_{V1a}	T_{V2a}	T_{V1a}	T_{V2a}	T_{V3a}	

Fig. 10. Spin–spin splitting of the ground and excited $^4A_2$ states of V_{Si}^- in 4H and 6H SiC as obtained from ODMR [1] and EPR data. $k_{(1,2)}$ and h show the site assignment.

in 4H and 6H SiC obtained from ODMR data [1] and EPR data are summarized in Fig. 10.

7. Conclusion

In 6H SiC both V1(V1′) and V3(V3′) have small hexagonal splitting in the excited states $^4E(^4E(a_1^1a_1^1e^3)-^4A_2(a_1^1a_1^2e^2)$ whereas for V2 only the $^4A_2(a_1^1a_1^2e^2)$ excited state is visible indicating that V1(V1′) and V3(V3′) originate from the k_1 and k_2 sites, respectively, and V2 from the h site, (Figs. 5 and 10). This indication is further supported by the fact that the spin–spin splitting of the ground states $^4A_2(a_1^2a_1^1e^2)$ as well as of the excited states $^4A_2(a_1^1a_1^2e^2)$ are very similar for the k_1 and k_2 sites; the splitting of the excited states is larger than the splitting of the ground states. The h site is different; the spin–spin splitting of the ground state is very much larger than for the k_1 and k_2 sites whereas the splitting of the excited state is smaller. In analogy with 6H SiC V2 in 4H SiC originates from the h site and V1(V1′) from the k site.

8. Summary

We have proposed a model supported by calculations of the silicon vacancy in 4H and 6H SiC that explains the optical transitions and the magnetic resonance signals observed as occurring in the singly negative charge state. The assignment of the silicon vacancies at the different inequivalent sites is suggested.

Acknowledgments

The support from the Swedish Foundation for Strategic Research, the Swedish National Supercomputer Centre, ABB (South Africa), Advanced Laboratory Solutions, and the National Research Foundation (South Africa) is gratefully acknowledged.

References

[1] E. Sörman, N.T. Son, W.M. Chen, O. Kordina, C. Hallin, E. Janzén, Phys. Rev. B 61 (2000) 2613.
[2] M. Wagner, B. Magnusson, W.M. Chen, E. Janzén, E. Sörman, C. Hallin, J.L. Lindström, Phys. Rev. B 62 (2000) 16555.
[3] N. Mizuochi, S. Yamasaki, H. Takizawa, N. Morishita, T. Ohshima, H. Itoh J. Isoya, Phys. Rev. B 66 (2002) 235202.
[4] N. Mizuochi, S. Yamasaki, H. Takizawa, N. Morishita, T. Ohshima, H. Itoh T. Umeda, J. Isoya, Phys. Rev. B 72 (2005) 235208.
[5] S.B. Orlinski, J. Schmidt, E.N. Mokhov, P.G. Baranov, Phys. Rev. B 76 (2003) 125207.
[6] T. Wimbauer, B.K. Meyer, A. Hofstaetter, A. Scharmann, H. Overhof, Phys. Rev. B 56 (1997) 7384.
[7] H. Itoh, M. Yoshikawa, I. Nashiyama, S. Misawa, H. Okumura, S. Yoshida, IEEE Trans. Nucl. Sci. 37 (1990) 1732.